

The consequences of craniofacial integration for the adaptive radiations of Darwin's finches and Hawaiian honeycreepers

Guillermo Navalón^{1,2,3*}, Jesús Marugán-Lobón^{2,4}, Jen A. Bright⁵, Christopher R. Cooney^{1,6} and Emily J. Rayfield^{1*}

The diversifications of Darwin's finches and Hawaiian honeycreepers are two text-book examples of adaptive radiation in birds. Why these two bird groups radiated while the remaining endemic birds in these two archipelagos exhibit relatively low diversity and disparity remains unexplained. Ecological factors have failed to provide a convincing answer to this phenomenon, and some intrinsic causes connected to craniofacial evolution have been hypothesized. The tight coevolution of the beak and the remainder of the skull in diurnal raptors and parrots suggests that integration may be the prevalent condition in landbirds (Inopinaves). This is in contrast with the archetypal relationship between beak shape and ecology in Darwin's finches and Hawaiian honeycreepers, which suggests that the beak can adapt as a distinct module in these birds. Modularity has therefore been proposed to underpin the adaptive radiation of these groups, allowing the beak to evolve more rapidly and freely in response to ecological opportunity. Here, using geometric morphometrics and phylogenetic comparative methods in a broad sample of landbird skulls, we show that craniofacial evolution in Darwin's finches and Hawaiian honeycreepers seems to be characterized by a tighter coevolution of the beak and the rest of the skull (cranial integration) than in most landbird lineages, with rapid and extreme morphological evolution of both skull regions along constrained directions of phenotypic space. These patterns are unique among landbirds, including other sympatric island radiations, and therefore counter previous hypotheses by showing that tighter cranial integration, not only modularity, can facilitate evolution along adaptive directions.

Why some lineages diversify more or less than others is a central topic in evolutionary biology. Among birds, the adaptive island radiations of Darwin's finches and Hawaiian honeycreepers are notable for their rapid and disparate evolution^{1,2}. These clades quickly evolved to become taxonomically and morphologically more diverse than other avian lineages that colonized the same oceanic archipelagos^{3–7}. Since these phenomena were first recognized^{8,9}, many causal hypotheses have been proposed to explain such rapid island radiations. Extrinsic causes, such as differences in colonization age, have been largely dismissed because other slower-evolving lineages of birds colonized the archipelagos at similar times^{3–5,10}. Intrinsic explanations may offer more insight^{4,5,11,12}. In silico simulations and empirical studies show that the covariation structures of sets of characters (produced by genetic, developmental, functional or evolutionary causes) have important influences on phenotypic evolution (Fig. 1) (see refs. ^{13–15}). For example, simulations show that if an anatomical structure is integrated (that is, its component parts coevolve; see ref. ¹⁶), its phenotypic evolution will be constrained along specific lines within the trait space. Modularity (weaker integration between component parts), in turn, allows a less constrained exploration of trait space^{13,17} (Fig. 1a). A more modular organization is therefore traditionally believed to facilitate, or even to be a precondition¹⁸ for, evolvability¹⁹ by allowing component parts to evolve and adapt more independently from each other^{20,21}. An alternative view is that integration may enhance evolvability by providing an adaptive line of least

resistance, along which species may rapidly evolve, albeit within a constrained region of trait space^{13,17,22–24} (Fig. 1c). Although the degree to which integration and modularity affect evolution seems to be controlled by selection, some empirical discrepancies still exist^{13,17,22–24}. It might be expected that birds, a speciose vertebrate group with extremely divergent beak shapes, demonstrate little covariation between the beak and the remainder of the skull. This holds true at a broad macroevolutionary level, and the beak evolved as a semi-independent structure displaying weak integration with the rest of the skull, arguably explaining its evolutionary plasticity²⁵. Yet, when integration is quantified at the family or subfamily level, studies have shown strong integration between the beak and skull morphology in diurnal raptors and parrots^{11,26}. Raptors and parrots occupy key phylogenetic positions at the base of the landbird (Inopinaves) radiation and within this radiation, respectively^{27–29} (Inopinaves also includes Darwin's finches and Hawaiian honeycreepers), suggesting that strong cranial integration might be ancestral to and prevalent in landbirds^{11,26}. While there is no inherent reason that selection on the shape of the beak would not also lead to adaptive changes in the shape of cranium, strong cranial integration within these clades has been suggested to reflect pleiotropic interactions among cranial regions that hamper a fine adaptation of beak shape to feeding ecology^{11,26}. This is in contrast with the paradigmatic relationship between feeding ecology and beak size and shape evolution in Darwin's finches^{30,31} and Hawaiian honeycreepers^{3,32}, which suggests that the beak in these clades is able to respond

¹School of Earth Sciences, University of Bristol, Bristol, UK. ²Unidad de Paleontología, Departamento de Biología, Universidad Autónoma de Madrid, Madrid, Spain. ³Department of Earth Sciences, University of Oxford, Oxford, UK. ⁴Dinosaur Institute, Natural History Museum of Los Angeles County, Los Angeles, CA, USA. ⁵Department of Biological and Marine Sciences, University of Hull, Hull, UK. ⁶Department of Animal and Plant Sciences, University of Sheffield, Sheffield, UK. *e-mail: guillermo.navalon@earth.ox.ac.uk; e.rayfield@bristol.ac.uk

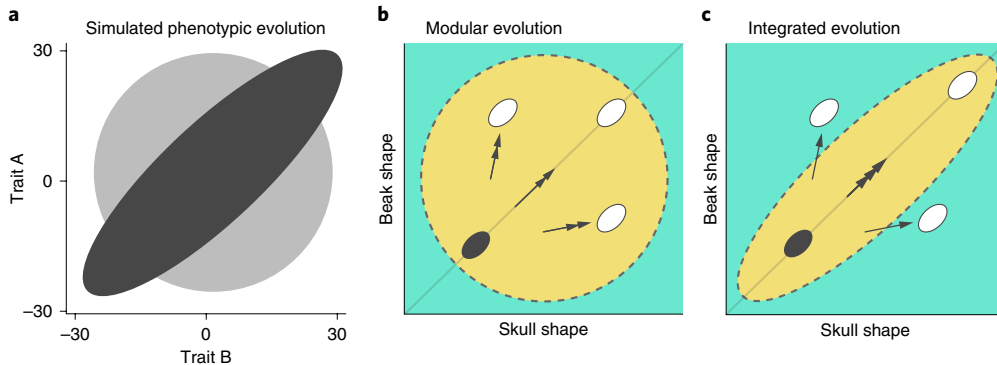


Fig. 1 | How integration and selection direct phenotypic evolution. **a**, Approximate areas of simulated phenotypic evolution for high (dark-grey ellipse) and zero (light-grey circle) trait covariation (modified from ref. ¹³). Higher integration entails the exploration of more extreme trait values (following ref. ¹⁷). **b**, A complete modular organization between beak and skull shapes (that is, zero covariation) represents the extreme scenario of the condition proposed for the classic passerine adaptive radiations whereby the beak can evolve more freely^{7,11,12}. This scenario permits the initial theoretical phenotype (dark-grey ellipse) to reach all three theoretical adaptive peaks (white ellipses), allowing greater evolutionary flexibility (for example, see refs. ^{13,74}). **c**, The alternative scenario, an integrated organization between beak and skull shapes (that is, stronger covariation), strongly facilitates reaching the theoretical adaptive peak that is aligned with the axis of maximum phenotypic covariance (that is, the phenotypic line of least resistance, sensu ref. ²³), to the detriment of the adaptive peaks that are not aligned with this axis^{17,23,24}. The boundary lines in **b** and **c** are dashed to reflect that phenotypic evolution is more likely to happen within the area described by the covariation structure (yellow area) but can occur beyond those limits (turquoise background), for instance if directional selection is strong enough (for example, see ref. ⁷⁵). The number of arrowheads in **b** and **c** represents the inferred speed of change when selection favours phenotypic evolution in that direction.

effectively and more or less independently to selective pressures from feeding in their island ecosystems (an observation that was crucial to developing the theory of natural selection^{8,33}). A key question, therefore, is whether the relaxation of cranial integration represents an evolutionary innovation in these landbird clades whereby the beak is able to evolve more freely, thus facilitating rapid evolutionary radiation^{11,12}, or whether integration facilitates rapid evolution along constrained adaptive directions. The recent surge of interest in the implications of integration and modularity for evolvability in evolutionary theory^{11,13,15,25,34} makes testing these ideas in an iconic example of adaptive radiation particularly relevant. Here, we use geometric morphometrics and phylogenetic comparative methods to quantify whether relaxed integration (modularity) between the beak and the skull is linked to rapid and disparate evolutionary radiation in landbirds as per classic interpretations, or whether tighter integration may be key to rapid and large evolutionary change.

Results and discussion

We found that each of the major clades of landbirds diverged to unique cranial morphologies (Fig. 2, Extended Data Figs. 3–5). Parrots (Psittaciformes) are characterized by a single ancestral shift towards very high rates of skull shape evolution, resulting in a characteristic cranial anatomy with short, curved beaks and expanded braincases (Fig. 2). Conversely, hoopoes and hornbills (Bucerotiformes) and toucans (Ramphastidae, Piciformes) show similar skull shapes to parrots but have less curved beaks with higher aspect ratios (Extended Data Figs. 3–5). While passerines (Passeriformes) have radiated to explore a large proportion of landbird morphological variation, they have not achieved the levels of morphological variation seen in non-passerines (Fig. 2). Although most passerines display similar skull morphologies and there is a slowdown in the rates of skull shape evolution in the branch leading to the songbirds (Passeri), a few songbird lineages diverge substantially to explore morphologies approaching those of parrots or hoopoes (Fig. 2, Extended Data Figs. 3–5). Darwin's finches and Hawaiian honeycreepers show the highest rates of beak and skull shape evolution in our sample, and experienced multiple positive rate shifts within each clade. This result is similar to those of other recent studies^{2,25}, suggesting that the rapidity of evolution in these

species is not simply a consequence of their recent divergence relative to the other species in our data. These birds also show considerable craniofacial shape disparity, including some of the most extreme shapes within Passeriformes (Fig. 2).

We found that the beak and the skull are integrated to an extent in all landbird clades (Figs. 3a and 4a). When considered as separate groups, Passeriformes have more integrated skulls than non-passerines (Fig. 4a, Table 1). This is driven by high integration in the songbirds (Passeri), moderately high integration in the suboscine passerines (Tyranni) within the Passeriformes and high integration in the parrots (Psittaciformes) within the non-passerines (Figs. 3a and 4a, Table 1, Extended Data Fig. 10). All other clades show lower and similar levels of cranial integration (Figs. 3a and 4a; Table 1). Within songbirds (Fig. 4b), Passerida, the clade containing Darwin's finches and Hawaiian honeycreepers, exhibits higher levels of integration than all other passerine clades and this probably underscores the high integration displayed by songbirds as a whole group. Interestingly, the Muscicapida, the other passerine clade that radiated in Galapagos and Hawaii (but to a lesser extent than Darwin's finches and Hawaiian honeycreepers), display the lowest levels of integration in our sample (Figs. 3b and 4b, Table 1). High levels of integration and the same pattern of covariation persist in Passerida even when Darwin's finches and Hawaiian honeycreepers are removed from the analysis (Figs. 3b and 4b; see Supplementary Figs. 5 and 6, Extended Data Fig. 10 and Supplementary Data Tables 1 and 2 for the congruence of these results with other analytical conditions), suggesting that craniofacial covariation in these clades matches the general covariation pattern of Passerida, indicating that high cranial integration may be more widespread in this clade. Therefore, contrary to previous suggestions, our results show that cranial evolution in the classic adaptive radiations of Darwin's finches and Hawaiian honeycreepers was most probably characterized by a pattern of strong integration between the beak and the rest of the skull.

Although there is no common relationship between the strength of cranial integration and rates of morphological evolution for all landbirds in our data (Extended Data Fig. 8), this matches expectations as recent in silico models and empirical data show that this relationship is also critically dependent on selection

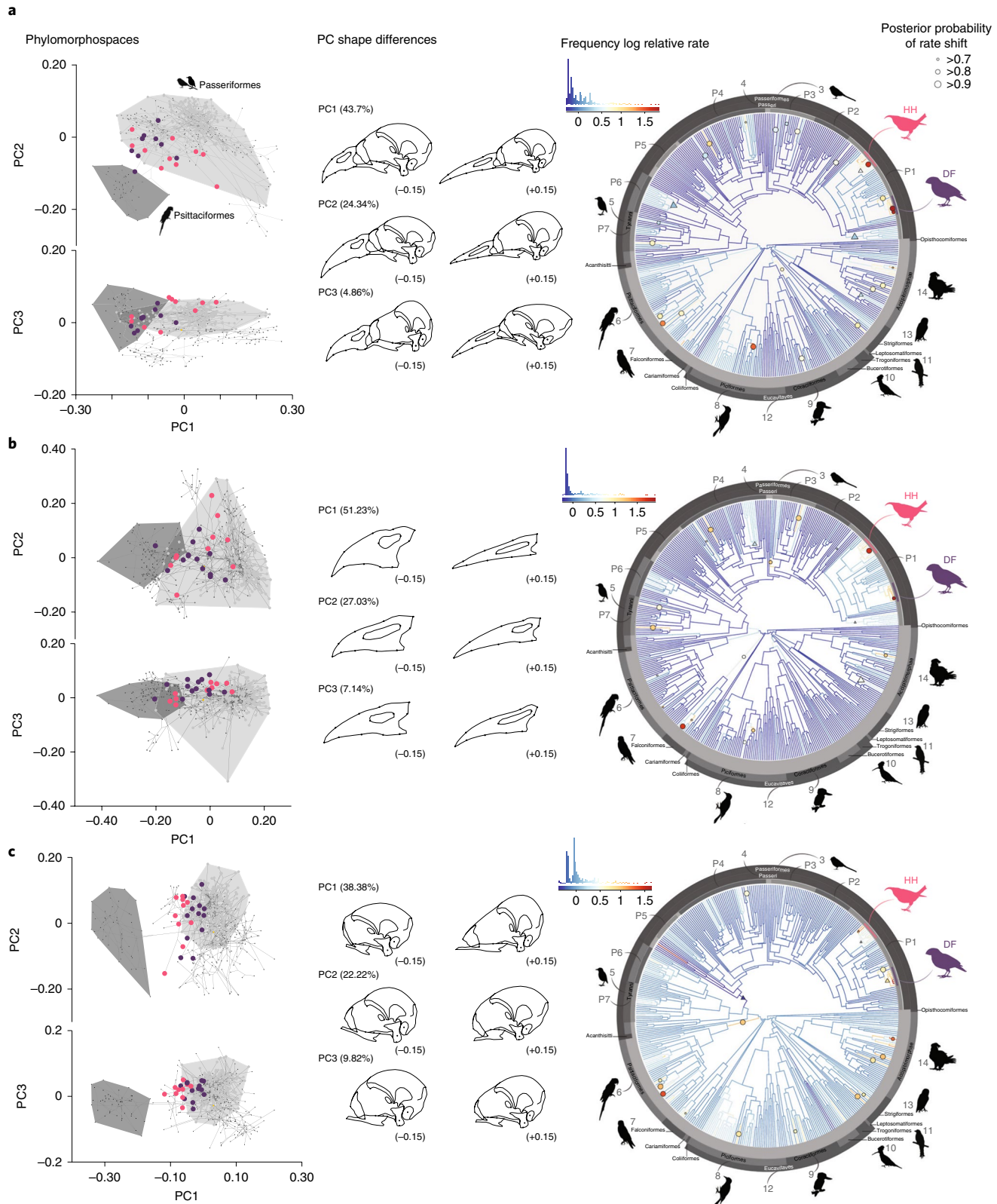


Fig. 2 | Pattern and tempo of craniofacial evolution in landbirds. **a–c**, Phylomorphospaces of the first three principal components (PCs) of shape (left), shape changes associated with these shape axes (centre) and rates of morphological evolution (right) for the whole skull (**a**), the beak block (**b**) and the skull block (**c**). The light-grey convex hull encloses Passeriformes, and the dark-grey convex hull encloses Psittaciformes. Purple dots represent Darwin's finches, and pink dots represent Hawaiian honeycreepers (see Extended Data Figs. 3–5 for the main landbird orders labelled in the phylomorphospaces). The branch colours in the phylogenies indicate the relative rates of evolution. Inferred rate shifts with higher posterior probabilities than 0.7 are plotted in corresponding branches (circles) or nodes (triangles) in the phylogeny (see Supplementary Tables 1–3 for the full list of rate shifts). The posterior probability of each inferred rate shift is indicated by the size of said circle or triangle. Histograms with the frequencies of log-transformed relative rates of morphological evolution are provided next to each phylogeny. Clade labels are the same as in Figs. 3 and 4 and Table 1. DF, Darwin's finches; HH, Hawaiian honeycreepers.

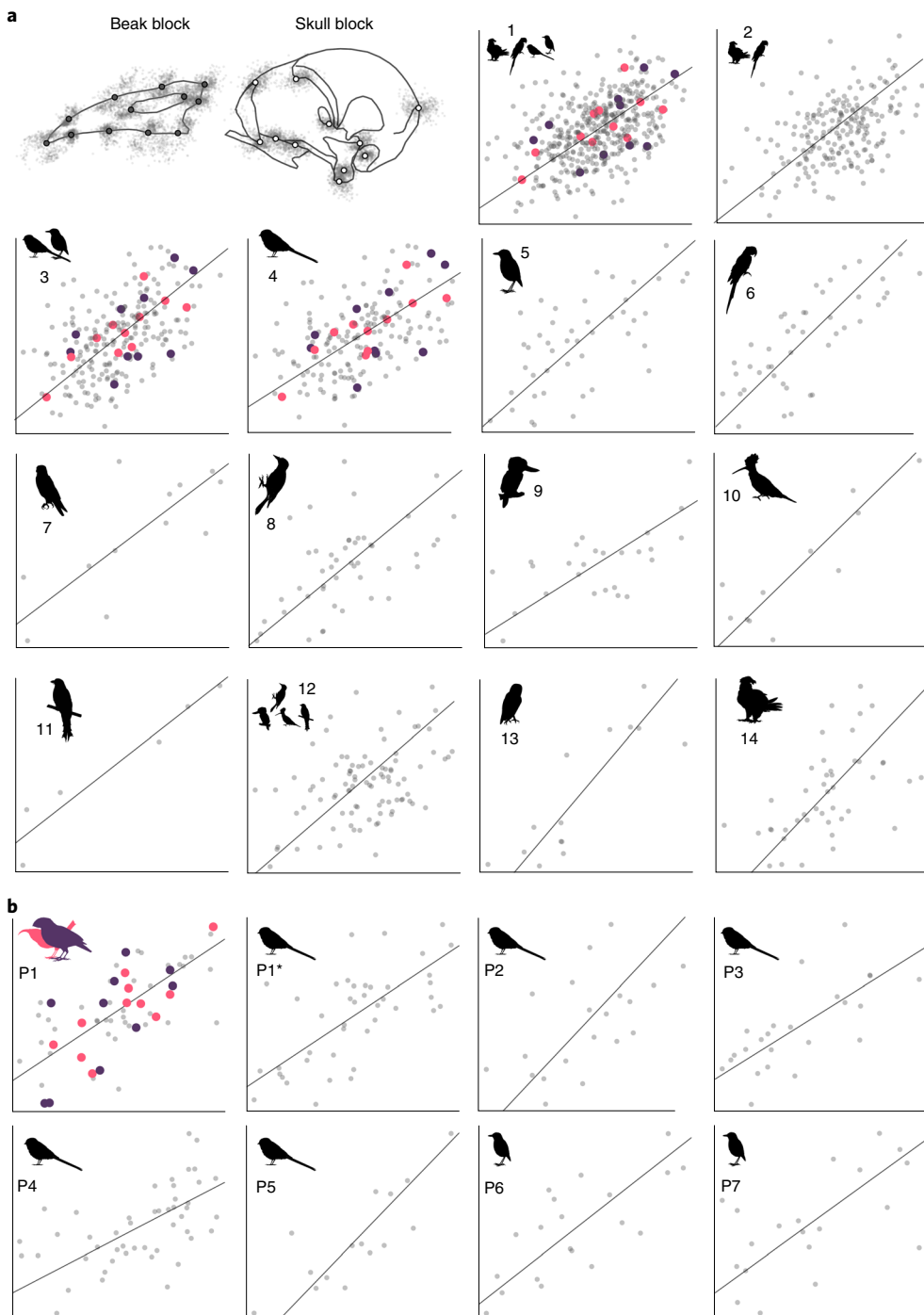


Fig. 3 | Evolutionary integration between the beak and the skull in landbirds. **a,b**, PLS1 plots for the two-block phylogenetic partial least squares (P-PLS) analyses using the rate-scaled phylogeny (situation 2, see Methods) in each clade (numbers correspond to clades as detailed in Table 1). The y axes show PLS1 scores for the beak block; the x axes show PLS1 scores for the skull block. Major landbird lineages are shown in **a**, and major passerine lineages are shown in **b**. Purple dots represent Darwin's finches; pink dots represent Hawaiian honeycreepers.

impinging on functional and developmental factors^{15,17,23,24,35}. Specifically, evolution along phenotypic lines of least resistance²³ predicts that, by affecting several traits in unison, higher trait covariation can increase evolutionary rates if selection favours evolutionary change along the line of maximum covariation^{17,23,24}, allowing more extreme morphologies to be explored^{13,36}. Therefore, the lack of correlation in an older lineage such as parrots (~30 million years ago (Ma) crown-group Psittaciformes²⁹) may be due to clade age: this lineage has been affected by multidirectional

selective pressures during its long evolution, complicating the identification of a straightforward relationship between strong evolutionary integration of the skull and phenotypic evolution (that is, the fly-in-a-tube model¹⁵). Conversely, Darwin's finches and Hawaiian honeycreepers (and sympatric contemporaneous radiations) are much younger clades (Fig. 4c), and are geographically restricted to their islands; they therefore represent a rare opportunity to make more detailed inferences of phenotypic evolution. Relaxed selection in island ecosystems is often invoked as resulting from

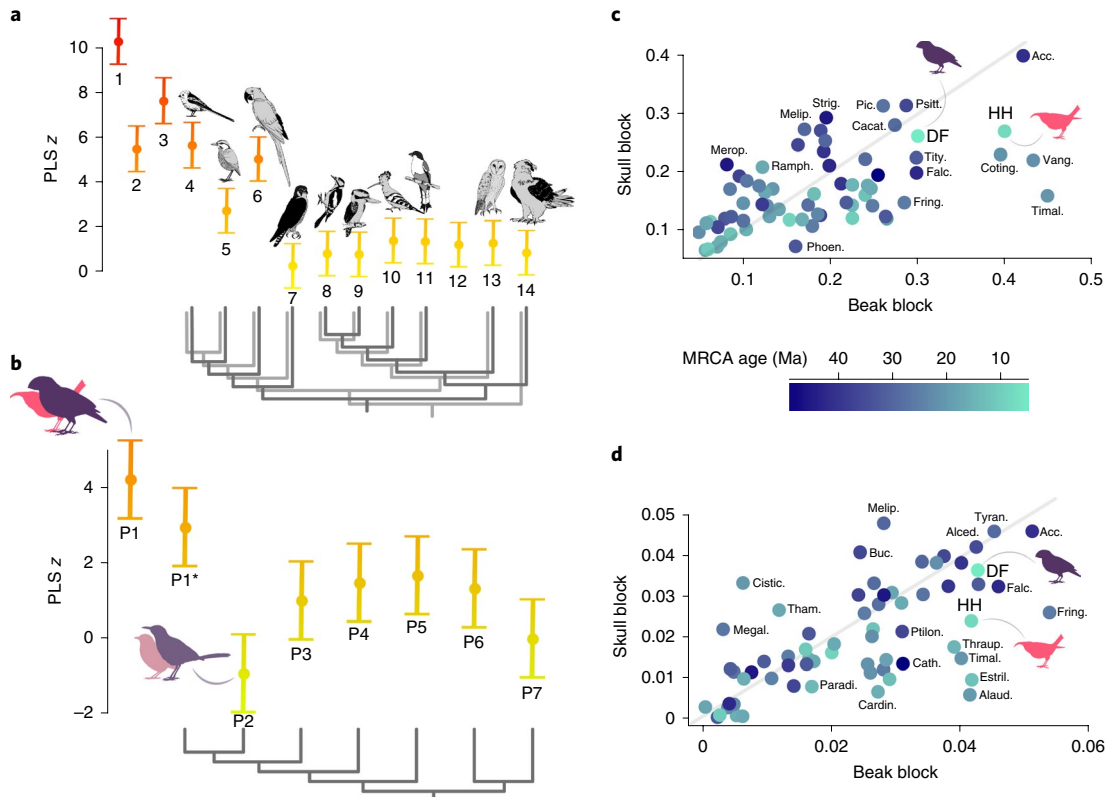


Fig. 4 | Strength of cranial integration across landbirds and maximum phenotypic distance in each family or subfamily. **a,b,** The z scores and corresponding confidence intervals for each major lineage of landbirds (**a**) and passerine parvorder (**b**). The z scores are the effect sizes from the randomized distribution of P-PLS correlation values (r_{PLS}) from the P-PLS for each clade (situation 2, two blocks, using the rate-scaled phylogeny; see Methods). The cladograms portray the simplified phylogenetic relationships of the main landbird lineages in our phylogeny (dark grey) compared with other recently published phylogenetic hypotheses²⁹ (light grey). In **b**, brighter silhouettes represent the island passeroids Darwin's finches (purple) and Hawaiian honeycreepers (pink), whereas paler silhouettes represent the island muscicapoids that radiated in the Galapagos (greyish purple) and Hawaii (greyish pink). Our phylogeny matches that of Prum et al.²⁹ for the interrelationships of major passerine lineages. **c,d,** Maximum total Procrustes distances for each family or subfamily for the beak and skull blocks. **d**, Maximum PLS1 distances for each family or subfamily for the beak and skull blocks. Labels in **c** and **d** correspond to families detailed in Extended Data Fig. 9. The colours of the dots in **c** and **d** correspond to the ages of the most recent common ancestor (MRCA) for each of the focal families in our maximum clade credibility (MCC) tree.

the availability of empty niche space and the scarcity of predators, particularly in newly colonized islands (that is, the island rule^{37,38}). Although this selection regime is often linked to divergent evolution³⁷, it may also facilitate evolution along lines of least resistance by raising the probability that selection favours change along adaptive phenotypic pathways. Although adaptive peaks can arise in more areas of trait space if selection is more flexible (therefore allowing more directions of evolution), the most likely change will by definition be the one using the line of least resistance (Fig. 1). For example, evolution along an allometric line of least resistance rather than divergent evolution may have facilitated the repeated evolution of phyletic dwarfism in island elephants³⁹. In a similar way, the constrained evolution of extreme morphologies along the maximum covariation line in Darwin's finches and Hawaiian honeycreepers might have favoured both rapid allopatric speciation and rapid niche separation by character displacement in each of the families because selection facilitating change in one cranial trait affected a cascade of other cranial regions³⁷. This, in turn, might underlie the comparatively higher rates of morphological evolution for the whole skull, and for both the beak and skull individually (Fig. 2, Supplementary Table 1–3; see also refs. ^{2,25}). In agreement with this model, we show that at the family or subfamily level, Darwin's finches and Hawaiian honeycreepers exhibit some of the most extreme shape differences along the axis of maximum

covariation between the beak and skull shapes (the purported phenotypic line of least resistance; see Methods) for the passeroid songbirds (Passerida) (Extended Data Fig. 7) and for all songbirds (Fig. 4c). This coordinated phenotypic evolution (Extended Data Fig. 6) might also be biomechanically important, as the jaw adductor muscles attach exclusively to the braincase block, yet act to power the beak during forceful biting. Increased integration between the beak and braincase may therefore facilitate improved feeding performance in both the beak and the rest of the skull in Hawaiian honeycreepers and in Darwin's finches, for whom a demonstrated link between beak morphology and feeding exists⁴⁰. This directional evolution may also have produced some of the highest values of total craniofacial disparity at the family or subfamily level for both clades (Fig. 4b), which is particularly striking considering that Darwin's finches and Hawaiian honeycreepers are substantially younger than most of the other families analysed (Fig. 4c). Therefore, the constrained (Figs. 3 and 4b,d, Table 1, Extended Data Fig. 7) but morphologically extreme (Figs. 2 and 4c) and rapid (Fig. 2) craniofacial evolution in Darwin's finches and Hawaiian honeycreepers meets the expectations of rapid evolution along lines of phenotypic least resistance^{17,23}, where high integration, rather than high modularity, facilitates evolution along a particular adaptive morphoclone.

Rapid evolution along lines of phenotypic least resistance may also explain the apparent contradiction between large phenotypic

Table 1 | Pairwise comparisons of z scores between clades and associated P values for situation 2**Main landbird lineages**

Mean z score	Clades	1	2	3	4	5	6	7	8	9	10	11	12	13
10.25	1. All landbirds													
5.47	2. Non-passerines	0.0196												
7.62	3. Passeriformes	0.4057	0.0245											
5.63	4. Passeri	0.2287	0.1715	0.1986										
2.71	5. Tyranni	0.0943	0.4649	0.0847	0.2324									
5.03	6. Psittaciformes	0.2087	0.0250	0.2683	0.1147	0.0532								
0.24	7. Falconiformes	0.0016	0.0301	0.0017	0.0091	0.0642	0.0015							
0.80	8. Piciformes	0.0003	0.0237	0.0005	0.0052	0.0720	0.0008	0.3873						
0.76	9. Coraciiformes	0.0033	0.0584	0.0034	0.0182	0.1103	0.0031	0.3675	0.4652					
1.38	10. Bucerotiformes	0.0183	0.1643	0.0172	0.0642	0.2292	0.0125	0.2224	0.2814	0.3272				
1.36	11. Trogoniformes	0.0083	0.1189	0.0083	0.0402	0.1885	0.0069	0.2420	0.3087	0.3564	0.4609			
1.21	12. Eucativataves	0.0001	0.0165	0.0001	0.0029	0.0719	0.0004	0.3380	0.4453	0.4898	0.3074	0.3389		
1.26	13. Strigiformes	0.0071	0.1066	0.0071	0.0354	0.1740	0.0061	0.2598	0.3318	0.3781	0.4391	0.4769	0.3648	
0.83	14. Accipitriformes	0.0008	0.0345	0.0010	0.0086	0.0865	0.0013	0.3716	0.4775	0.4862	0.3038	0.3326	0.4718	0.3556

Main passerine lineages

Mean z score	Clades	P1	P1*	P2	P3	P4	P5	P6
4.22	P1. Passerida							
2.95	P1*. Passerida*	0.2589						
-0.92	P2. Muscicapida	0.0004	0.0042					
1.01	P3. Sylviida	0.0310	0.1133	0.0853				
1.48	P4. Corvides	0.0344	0.1352	0.0483	0.4225			
1.66	P5. Meliphagoidea	0.1284	0.2916	0.0321	0.2881	0.3401		
1.33	P6. Tyrannida	0.0635	0.1838	0.0544	0.3956	0.4631	0.3831	
0.00	P7. Furnariida	0.0053	0.0287	0.2609	0.2431	0.1755	0.1143	0.1739

Bold values are statistically significant ($P < 0.05$). The z score for each clade is provided. P1*. Passerida* indicates Passerida excluding Darwin's finches and Hawaiian honeycreepers.

divergence and little change in genetic divergence between species in Darwin's finches and in Hawaiian honeycreepers^{3,5}. It may also shed some light on why other passerine lineages that colonized both archipelagos at similar times failed to undergo the same explosive adaptive radiation. In Hawaii, the two endemic lineages of passerine birds that colonized the archipelago at similar times to Hawaiian honeycreepers are the Hawaiian thrushes (five species, Turdidae)⁵ and the extinct Hawaiian honeyeaters (five species, Mohoidae)¹⁰. Both families belong to the parvorder Muscicapida, the passerine lineage exhibiting the lowest integration in our data (Fig. 4a). Similarly, the other endemic radiation in the Galapagos archipelago, the Galapagos mockingbirds (four species, Mimidae, also in the Muscicapida), colonized the islands at a similar time but did not undergo a rapid diversification⁴. While multiple ecologically relevant traits of the colonizer species may have contributed to the diversification patterns of passersines in Galapagos and Hawaii, we suggest that their lower craniofacial integration may have been an important factor preventing them exploiting adaptive lines of least resistance that probably produced the rapid and large evolutionary change in cranial morphology that we showed in Darwin's finches and Hawaiian honeycreepers. Nonetheless, our study demonstrates that adaptive radiations are possible under tighter cranial integration.

In summary, we propose that a stronger craniofacial integration was a key factor shaping the extreme craniofacial evolution of two classic radiations of island passeroids. While an intrinsic evolutionary lability of the beak has been proposed for several families of

passeroid songbirds^{5,31,32,40}, other studies have shown that beak shape in the group is constrained to a small series of shape transformations arising from a constrained morphogenetic program⁴¹. Our hypothesis reconciles both views by showing that although high cranial integration constrains the shapes of the beak and skull, it may also facilitate evolutionary lability along specific phenotypic clines in particular ecological scenarios.

Methods

Database and phylogenetic hypothesis. Our study includes 128 families of landbirds (that is, Inopinaves, defined as Telluraves⁴² + *Opisthocomus hoazin*²⁹), giving a total of 436 species (Supplementary Data Table 5). All but five families within the landbird radiation are represented in our sample. These families (Philepittidae, Sapayoaidae, Dasyornithidae, Urocynchramidae and Aegithinidae) are either monotypic or have an extremely reduced diversity, and are often regarded as belonging within other passerine families⁴³. Sampling was non-random and aimed to capture the maximum beak morphological disparity within each family, with a special focus on the subfamilies of Darwin's finches (Geospizinae) and Hawaiian honeycreepers (Drepanidinae) (represented in our sample by ~70% and ~60% of their extant diversity, respectively). A time-calibrated MCC phylogeny of the 436 species was generated using TreeAnnotator⁴⁴ from a population of 10,000 Hackett's backbone stage 2 trees. Trees were generated using the in-built tools from www.birdtree.org (for the full details of the tree construction methods, see ref. ¹), and branch lengths were set equal to 'Common ancestor' node heights. The resulting MCC phylogeny is largely congruent with the last genomic phylogenies for the interrelationships of landbirds (Figs. 2 and 4a,b; see refs. ^{28,29}).

Geometric morphometrics. A set of 17 landmarks and 2 curves (3 evenly separated semilandmarks along the dorsal and ventral rims of the beak) was digitized using the software tpsDig v.2.10 (ref. ⁴⁵) in lateral views of the skull of

each specimen (Extended Data Figs. 1 and 2). The minimum bending energy criterion was applied to slide the semilandmarks in tpsRelw v.1.69⁴⁶, as this is more appropriate than the minimum Procrustes distance criterion when dealing with data with high morphological variation in the software used here⁴⁷. Landmarks and semilandmarks were then classified as belonging to the beak block (block 1) or the skull block (block 2) (Extended Data Figs. 1 and 2). Shape data (Procrustes coordinates) were extracted using three full generalized Procrustes analyses (GPAs) for: (1) the whole landmark configuration, (2) the beak block and (3) the skull block. An additional generalized resistant Procrustes superimposition (GRPS)⁴⁸ was conducted in the raw coordinates from the whole landmark configuration to identify possible trait-correlation artefacts in our shape data (see Evolutionary covariation and Supplementary information). GPA aligned Procrustes coordinates were thereafter imported to MorphoJ v.1.06d⁴⁹ and the R statistical environment⁵⁰ for all downstream analyses.

Principal component analyses and variable rates model analyses. To explore the main patterns of skull shape variation in landbirds, we conducted principal component analyses (PCAs) for: (1) the whole configuration, (2) the beak block and (3) the skull block. The time-calibrated MCC phylogeny was mapped over the PCAs by weighted (that is, including branch length information) square-change parsimony to visualize evolutionary changes over the morphospace. PCAs (including mapping time calibrated trees) were conducted in MorphoJ.

To explore the tempo of craniofacial evolution in landbirds, we used the scores derived from the previous PCAs to conduct variable rates model analyses (VRMAs) using the software BayesTraits v.2.0.2 (ref. ⁵¹) (available from <http://www.evolution.rdg.ac.uk/>). This method uses a reversible jump Markov chain Monte Carlo approach to estimate the location, probability and magnitude of rate shifts in continuous traits across branches of a phylogenetic tree (see ref. ⁵²). We used PC scores for: (1) the whole skull (13 PCs), (2) the beak block (6 PCs) and (3) the skull block (10 PCs). We used the number of PCs that account for 95% of shape variance, except for the whole configuration where we used the number that account for 90% to avoid poor performance due to a high number of variables⁵³. We ran two replicate chains for each model using default priors and assuming uncorrelated trait axes⁵⁴. Each chain was run for 200,000,000 iterations (sampled every 10,000 iterations), with the first 100,000,000 iterations removed as burn in. We confirmed that replicate runs had converged and combined the outputs of both runs for further analysis. We summarized the results of each run by calculating the mean rate and the probability of a rate shift (branch or clade) over all posterior samples for each node in the tree. In the main text, we focus on rate shifts that are inferred with higher posterior probabilities than 0.70. To account for rate heterogeneity in the downstream analyses of evolutionary covariation (see Evolutionary covariation and Supplementary information), a rate-scaled phylogeny (non-ultrametric) was generated by using the branch lengths predicted by the model of the VRMA conducted with the whole skull configurations.

Evolutionary covariation. Evolutionary covariation between the beak block (block 1) and the skull block (block 2) was examined for each of the clades of landbirds by means of P-PLS analysis^{54,55} in three different situations: two blocks using the calibrated time tree (separate GPAs for the beak block and the skull block) (situation 1), two blocks using the rate-scaled phylogeny (situation 2) and one configuration (one single GPA for the whole configuration) using the rate-scaled tree (situation 3). P-PLS is a multivariate analysis that quantifies the evolutionary covariation between two sets of data by searching for vectors of correlated variables without implying predictability of one set of variables on the other.

Although least-squares GPA⁵⁶ provides a universal criterion for defining shape data, and convenient statistical properties for downstream multivariate analyses that other superimposition methods do not⁵⁷, it has some widely recognized limitations when shape differences between landmarks are highly heterogeneous^{48,58–60}. This is because GPA assumes that variation among landmarks is homogeneous and that all landmarks vary isotropically⁵⁶ (they are equally distributed in all directions). Therefore, if a great deal of the total shape difference is concentrated in just a few landmarks, and/or its variation is skewed towards one or more directions, GPA tends to spread this localized shape variance across the whole configuration, generating artefactual shape differences^{48,60–62} (that is, the Pinocchio effect⁶³). This issue can be particularly misleading when evaluating covariation patterns (that is, integration and modularity) as it tends to overestimate integration. There is still debate as to whether this is a critical concern in real biological data or not^{48,60,63}; however, in an exploratory study, Cardini⁶⁴ showed that GPA can generate artefactual patterns of covariation even if the original shape data exhibit no covariation at all. The fact that landbirds demonstrate high beak shape variation relative to other skull regions^{25,34} led us to contemplate this possibility. Therefore, to identify whether the aforementioned might be a problem in our sample, we carried out a GRPS^{48,59} in the raw coordinates (unaligned) for the whole configurations for all landbirds and compared them with a GPA superimposition using Resistant Procrustes Software v.1.0⁴⁸ (available online at <https://sites.google.com/site/resistantprocrustes/>) (Supplementary Fig. 4). GRPS differs from GPA in that the criteria for eliminating rotational information from shape data are estimated through a repeated-medians calculation for each dataset, rather than minimizing the squared sum of Euclidean distances between the

landmark coordinates⁵⁹. This criterion is therefore robust to larger variation in a few landmarks with respect to the whole configuration, and thus better portrays localized variation across coordinates^{48,59}. We also tested evolutionary shape covariation between blocks 1 and 2 within one configuration (situation 3) to gain insight on how localized variation might affect integration results in our sample (Extended results, Supplementary Figs. 5 and 6, Supplementary Table 2).

Because GRPS and other resistant-based procedures are not based on Procrustes distances, concerns have been expressed regarding their ability to generate shape tangent spaces appropriate for Euclidean multivariate statistics (for example, see ref. ⁶⁴). Although there are specifically implemented multivariate methods for dealing with data extracted from a GRPS, the standard usage of GPA in modern geometric morphometrics^{65,66} means that most available methods are based on Procrustes distances. These Procrustes-based analyses need the consistency with the Procrustes projection that defines shape variables in geometric morphometrics⁵⁷. To our knowledge, there is no appropriate method able to overcome trait correlation artefacts yet retain an equivalence with Euclidean multivariate statistics. We are therefore forced to quantify covariation using two blocks (situations 1 and 2) in an attempt to mitigate any artefactual spread of variance across the whole configuration (see Extended results for further details). This approach better portrays the original patterns of local variation in geometric morphometrics and generally eliminates artefactual trait covariation, at least as far as integration is concerned⁶⁰. However, covariation in situations 1 and 2 only reflects evolutionary shape covariation, as information regarding the relative size and arrangement between blocks is lost (eliminated in each block's separate GPA) and can only be accessed indirectly (for example, because the shape data is a two-dimensional projection of a three-dimensional object, certain shape changes might be indicative of differences in arrangement angle).

Several studies have shown that landbirds exhibit extreme heterogeneity in rates of craniofacial evolution^{2,25}, which we also quantified here (Fig. 2, Supplementary Tables 1–3). The computation of P-PLS in geomorph⁶⁷ assumes a single-rate Brownian motion (BM) model of evolution, which is unlikely to conform to shape data that evolved with highly heterogeneous rates. When shape data do not conform to a single-rate BM model, previous approaches rescaled the branch lengths of the phylogeny using the parameters estimated by the model that best fits the data from a selection of a priori models, namely: single-rate BM, Ornstein–Uhlenbeck and early-burst (for example, see ref. ⁶⁸). This approach coerces the phylogenetic covariation matrix to approximate a BM model, thereby meeting the expectations of the analysis. However, recent research has shown that current model-fitting methods based on maximum likelihood tend to exhibit ill-conditioned covariation matrices, leading to misidentifications of the model of evolution⁵³, even when the data are generated under a particular model like BM⁶⁹. Here, we chose a different approach: we used the branch lengths estimated by the VRMA for the whole skull configuration. In this way, we rescaled the branch lengths in our tree to account for the actual rates of phenotypic evolution rather than using parameters estimated by the fit to a particular set of a priori single-process models. Although this solution is not ideal, it allows for the inclusion of branch lengths estimated by more complex models than previous approaches, which have also been shown to exhibit best fits for other cases of trait evolution such as body mass⁷⁰. The methodological endeavour needed to implement more complex evolutionary models in phylogenetic comparative methods for high dimensional data⁷¹ goes well beyond the scope of this study. Here, comparisons between situations 1 and 2 aimed to gain insight on the effects of accounting for variable rates in evolutionary covariation in measures of evolutionary integration (Supplementary Figs. 2 and 3; Supplementary Data Table 3).

The strength of evolutionary covariation in each of the three scenarios was compared and tested between major radiations of landbirds and between the major radiations of passerines following a recently developed statistical procedure⁷². The major non-passerine radiations were compared with the major subdivisions of the Passeriformes (Passeri and Tyranni) on the basis of the high support in all the latest phylogenetic hypotheses of these clades and similar node age estimations²⁹. The more recently branching passerine parvorders were compared between each other. As r_{PLS} values have been shown to be influenced by sample size⁷³, comparing or testing for differences in integration levels between two different sample sizes using this statistic is problematic. Adams and Collyer⁷² recently proposed the use of r_{PLS} effects sizes (z scores). We therefore calculated z scores as the standard deviates of the r_{PLS} values from the permutation procedure for the P-PLS analyses of each clade, and we calculated confidence intervals for each value. Pairwise differences in z scores were then compared and statistically tested to discriminate between levels of integration between clades. We used z score values directly to elucidate which clades exhibited higher integration when differences were found. To explore the differences in the patterns of cranial integration between clades, pairwise angles and correlations of PLS1 vectors (the pair of vectors that covary most for each P-PLS) were calculated for all the clades in situation 2 (Extended Data Figs. 6 and 10, Supplementary Fig. 1, Supplementary Data Tables 1 and 2). Histograms of the frequencies of binned angles and shape differences across each vector were plotted for visual comparisons (Extended Data Fig. 6, Supplementary Fig. 1).

Finally, we addressed whether stronger cranial integration generated greater morphological change along the evolutionary line of least resistance in Darwin's finches and Hawaiian honeycreepers than in other landbird families.

To do so, we computed maximum distances within each family (or subfamily for Geospizinae and Drepanidinae) of landbirds for the PLS1 scores of the beak and skull blocks as a proxy of the degree of spread along the line of least resistance. We did this for the PLS1 axes defined for each order (and Passeri and Tyramni for the Passeriformes) and compared PLS1 distances for the beak and skull blocks between all the families. Furthermore, we repeated this procedure for the parvorder Passerida and compared PLS1 distances for the beak and skull blocks between passeroid families alone. To ascertain whether a larger spread across the lines of least resistance also corresponds to more extreme cranial morphologies, we computed maximum Procrustes distances within each family or subfamily using the Procrustes coordinates (both from the whole configuration and from the beak and skull blocks separately).

Reporting Summary. Further information on research design is available in the Nature Research Reporting Summary linked to this article.

Data availability

All relevant data are available via the University of Bristol's DataBris repository at <https://data.bris.ac.uk/data/dataset/3kpwgnqewcy2tak6uzzdzt>.

Received: 29 July 2019; Accepted: 17 December 2019;

Published online: 3 February 2020

References

- Jetz, W., Thomas, G., Joy, J., Hartmann, K. & Mooers, A. The global diversity of birds in space and time. *Nature* **491**, 444–448 (2012).
- Cooney, C. R. et al. Mega-evolutionary dynamics of the adaptive radiation of birds. *Nature* **542**, 344–347 (2017).
- Burns, K. J., Hackett, S. J. & Klein, N. K. Phylogenetic relationships and morphological diversity in Darwin's finches and their relatives. *Evolution* **56**, 1240–1252 (2002).
- Arbogast, B. S. et al. The origin and diversification of Galapagos mockingbirds. *Evolution* **60**, 370–382 (2006).
- Lovette, I. J., Bermingham, E. & Ricklefs, R. E. Clade-specific morphological diversification and adaptive radiation in Hawaiian songbirds. *Proc. R. Soc. Lond. B* **269**, 37–42 (2002).
- Pratt, H. D. & Conant, S. *The Hawaiian Honeycreepers: Drepanidinae* (Oxford Univ. Press, 2005).
- Tokita, M., Yano, W., James, H. F. & Abzhanov, A. Cranial shape evolution in adaptive radiations of birds: comparative morphometrics of Darwin's finches and Hawaiian honeycreepers. *Phil. Trans. R. Soc. B* **372**, 20150481 (2017).
- Darwin, C. *The Zoology of the Voyage of HMS Beagle: Under the Command of Captain Fitzroy, RN, During the Years 1832 to 1836: Published with the Approval of the Lords Commissioners of Her Majesty's Treasury* (Smith, Elder and Company, 1839).
- Mayr, E. The zoogeographic position of the Hawaiian Islands. *Condor* **45**, 45–48 (1943).
- Fleischer, R. C., James, H. F. & Olson, S. L. Convergent evolution of Hawaiian and Australo-Pacific honeyeaters from distant songbird ancestors. *Curr. Biol.* **18**, 1927–1931 (2008).
- Bright, J. A., Marugán-Lobón, J., Cobb, S. N. & Rayfield, E. J. The shapes of bird beaks are highly controlled by nondietary factors. *Proc. Natl Acad. Sci. USA* **113**, 5352–5357 (2016).
- Abzhanov, A. The old and new faces of morphology: the legacy of D'Arcy Thompson's 'theory of transformations' and 'laws of growth'. *Development* **144**, 4284–4297 (2017).
- Goswami, A., Smaers, J., Soligo, C. & Polly, P. The macroevolutionary consequences of phenotypic integration: from development to deep time. *Phil. Trans. R. Soc. B* **369**, 20130254 (2014).
- Klingenberg, C. P. Studying morphological integration and modularity at multiple levels: concepts and analysis. *Phil. Trans. R. Soc. B* **369**, 20130249 (2014).
- Felice, R. N., Randau, M. & Goswami, A. A fly in a tube: macroevolutionary expectations for integrated phenotypes. *Evolution* **72**, 2580–2594 (2018).
- Olson, E. C. & Miller, R. L. *Morphological Integration* (Univ. Chicago Press, 1999).
- Villmoare, B. Morphological integration, evolutionary constraints, and extinction: a computer simulation-based study. *Evol. Biol.* **40**, 76–83 (2013).
- Fisher, R. A. *The Genetic Theory of Natural Selection* (Dover, 1958).
- Kirschner, M. & Gerhart, J. Evolvability. *Proc. Natl Acad. Sci. USA* **95**, 8420–8427 (1998).
- Wagner, G. P. & Altenberg, L. Perspective: complex adaptations and the evolution of evolvability. *Evolution* **50**, 967–976 (1996).
- Raff, R. A. *The Shape of Life: Genes, Development, and the Evolution of Animal Form* (Univ. Chicago Press, 2012).
- Wagner, G. Coevolution of functionally constrained characters: prerequisites for adaptive versatility. *Biosystems* **17**, 51–55 (1984).
- Marroig, G. & Cheverud, J. M. Size as a line of least evolutionary resistance: diet and adaptive morphological radiation in New World monkeys. *Evolution* **59**, 1128–1142 (2005).
- Hansen, T. F. Is modularity necessary for evolvability? Remarks on the relationship between pleiotropy and evolvability. *Biosystems* **69**, 83–94 (2003).
- Felice, R. N. & Goswami, A. Developmental origins of mosaic evolution in the avian cranium. *Proc. Natl Acad. Sci. USA* **115**, 555–560 (2018).
- Bright, J. A., Marugán-Lobón, J., Rayfield, E. J. & Cobb, S. N. The multifactorial nature of beak and skull shape evolution in parrots and cockatoos (Psittaciformes). *BMC Evol. Biol.* **19**, 104 (2019).
- Hackett, S. J. et al. A phylogenomic study of birds reveals their evolutionary history. *Science* **320**, 1763–1768 (2008).
- Jarvis, E. D. et al. Whole-genome analyses resolve early branches in the tree of life of modern birds. *Science* **346**, 1320–1331 (2014).
- Prum, R. O. et al. A comprehensive phylogeny of birds (Aves) using targeted next-generation DNA sequencing. *Nature* **526**, 569–573 (2015).
- Gibbs, H. L. & Grant, P. R. Oscillating selection on Darwin's finches. *Nature* **327**, 511–513 (1987).
- Grant, P. R. & Grant, B. R. Evolution of character displacement in Darwin's finches. *Science* **313**, 224–226 (2006).
- Smith, T. B., Freed, L. A., Lepson, J. K. & Carothers, J. H. Evolutionary consequences of extinctions in populations of a Hawaiian honeycreeper. *Conserv. Biol.* **9**, 107–113 (1995).
- Darwin, C. & Wallace, A. On the tendency of species to form varieties; and on the perpetuation of varieties and species by natural means of selection. *Zool. J. Linn. Soc.* **3**, 45–62 (1858).
- Klingenberg, C. P. Cranial integration and modularity: insights into evolution and development from morphometric data. *Hystrix* **24**, 43–58 (2013).
- Schlüter, D. Adaptive radiation along genetic lines of least resistance. *Evolution* **50**, 1766–1774 (1996).
- Randau, M. & Goswami, A. Unravelling intravertebral integration, modularity and disparity in Felidae (Mammalia). *Evol. Dev.* **19**, 85–95 (2017).
- Losos, J. B. & Ricklefs, R. E. Adaptation and diversification on islands. *Nature* **457**, 830–836 (2009).
- Wright, N. A., Steadman, D. W. & Witt, C. C. Predictable evolution toward flightlessness in volant island birds. *Proc. Natl Acad. Sci. USA* **113**, 4765–4770 (2016).
- van der Geer, A. A., Lyras, G. A., Mitteroecker, P. & MacPhee, R. D. From Jumbo to Dumbo: cranial shape changes in elephants and hippos during phyletic dwarfing. *Evol. Biol.* **45**, 303–317 (2018).
- Grant, B. R. & Grant, P. R. Evolution of Darwin's finches caused by a rare climatic event. *Proc. R. Soc. Lond. B* **251**, 111–117 (1993).
- Fritz, J. A. et al. Shared developmental programme strongly constrains beak shape diversity in songbirds. *Nat. Commun.* **5**, 3700 (2014).
- Yuri, T. et al. Parsimony and model-based analyses of indels in avian nuclear genes reveal congruent and incongruent phylogenetic signals. *Biology* **2**, 419–444 (2013).
- Del Hoyo, J. et al. *Handbook of the Birds of the World Alive* (Lynx Editions, 2017).
- Rambaut, A. & Drummond, A. TreeAnnotator v1.7.0 (2013); <http://beast.community/treeannotator.html>
- Rohlf, F. tpsDig v2.10 (Department of Ecology and Evolution, State Univ. New York at Stony Brook, 2006).
- Rohlf, F. tpsRelw, relative warps analysis (Department of Ecology and Evolution, State Univ. New York at Stony Brook, 2010).
- Perez, S. I., Bernal, V. & Gonzalez, P. N. Differences between sliding semi-landmark methods in geometric morphometrics, with an application to human craniofacial and dental variation. *J. Anat.* **208**, 769–784 (2006).
- Torcida, S., Perez, S. I. & Gonzalez, P. N. An integrated approach for landmark-based resistant shape analysis in 3D. *Evol. Biol.* **41**, 351–366 (2014).
- Klingenberg, C. MorphoJ: an integrated software package for geometric morphometrics. *Mol. Ecol. Resour.* **11**, 353–357 (2011).
- R Core Team *R: A Language and Environment for Statistical Computing* (R Foundation for Statistical Computing, 2017); <http://www.R-project.org/>
- Pagel, M. & Meade, A. BayesTraits v2.0 (Univ. Reading, 2013).
- Venditti, C., Meade, A. & Pagel, M. Multiple routes to mammalian diversity. *Nature* **479**, 393–396 (2011).
- Adams, D. C. & Collyer, M. L. Multivariate phylogenetic comparative methods: evaluations, comparisons, and recommendations. *Syst. Biol.* **67**, 14–31 (2017).
- Adams, D. C. & Felice, R. N. Assessing trait covariation and morphological integration on phylogenies using evolutionary covariance matrices. *PLoS ONE* **9**, e94335 (2014).
- Rohlf, F. J. & Corti, M. Use of two-block partial least-squares to study covariation in shape. *Syst. Biol.* **49**, 740–753 (2000).
- Rohlf, F. J. & Slice, D. Extensions of the Procrustes method for the optimal superimposition of landmarks. *Syst. Biol.* **39**, 40–59 (1990).
- Bookstein, F. L. in *Advances in Morphometrics. NATO ASI Series (Series A: Life Sciences)* Vol. 284 (eds Marcus, L. F. et al.) 131–151 (Springer, 1996).

58. Dryden, I. & Mardia, K. *Statistical Analysis of Shape* (Wiley, 1998).
59. Siegel, A. F. & Benson, R. H. A robust comparison of biological shapes. *Biometrics* **38**, 341–350 (1982).
60. Cardini, A. Integration and modularity in Procrustes shape data: is there a risk of spurious results? *Evol. Biol.* **46**, 90–105 (2018).
61. Chapman, R. E. Conventional procrustes approaches. In *Proc. of the Michigan Morphometrics Workshop* Vol. 2 (eds Rohlf, F. J. & Bookstein, F.) 251–267 (Univ. Michigan Museum of Zoology, 1990).
62. Zelditch, M. L., Swiderski, D. L. & Sheets, H. D. *Geometric Morphometrics for Biologists: A Primer* (Academic, 2012).
63. Klingenberg, C. P. & McIntyre, G. S. Geometric morphometrics of developmental instability: analyzing patterns of fluctuating asymmetry with Procrustes methods. *Evolution* **52**, 1363–1375 (1998).
64. Bookstein, F. L. in *Image Fusion and Shape Variability Techniques: Proceedings* (eds Gill, C. A. & Mardia, K. V.) 59–70 (Leeds University Press, 1996).
65. Adams, D. C., Rohlf, F. J. & Slice, D. E. A field comes of age: geometric morphometrics in the 21st century. *Hystrix* **24**, 7–14 (2013).
66. Adams, D. C., Rohlf, F. J. & Slice, D. E. Geometric morphometrics: ten years of progress following the ‘revolution’. *Ital. J. Zool.* **71**, 5–16 (2004).
67. Adams, D. C., Collyer, M. L. & Kaliontzopoulou, A. Geomorph: software for geometric morphometric analyses. R package version 3.0.7 (2018); <https://cran.r-project.org/package=geomorph>
68. Zelditch, M. L., Ye, J., Mitchell, J. S. & Swiderski, D. L. Rare ecomorphological convergence on a complex adaptive landscape: body size and diet mediate evolution of jaw shape in squirrels (Sciuridae). *Evolution* **71**, 633–649 (2017).
69. Uyeda, J. C., Caetano, D. S. & Pennell, M. W. Comparative analysis of principal components can be misleading. *Syst. Biol.* **64**, 677–689 (2015).
70. Chira, A. M. & Thomas, G. H. The impact of rate heterogeneity on inference of phylogenetic models of trait evolution. *J. Evol. Biol.* **29**, 2502–2518 (2016).
71. Monteiro, L. R. Morphometrics and the comparative method: studying the evolution of biological shape. *Hystrix* **24**, 25–32 (2013).
72. Adams, D. C. & Collyer, M. L. On the comparison of the strength of morphological integration across morphometric datasets. *Evolution* **70**, 2623–2631 (2016).
73. Mitteroecker, P. & Bookstein, F. The conceptual and statistical relationship between modularity and morphological integration. *Syst. Biol.* **56**, 818–836 (2007).
74. Marroig, G., Shirai, L. T., Porto, A., de Oliveira, F. B. & De Conto, V. The evolution of modularity in the mammalian skull II: evolutionary consequences. *Evol. Biol.* **36**, 136–148 (2009).
75. Renaud, S., Auffray, J. C. & Michaux, J. Conserved phenotypic variation patterns, evolution along lines of least resistance, and departure due to selection in fossil rodents. *Evolution* **60**, 1701–1717 (2006).

Acknowledgements

We thank J. Cooper and J. White (NHM Tring), and C. M. Milensky and B. K. Schmidt (Smithsonian National Museum of Natural History) for access to specimens. We thank F. Blanco, M. Fabbri, I. Menéndez and L. Porras for discussions on the evolutionary implications of this research. We thank G. Thomas, T. Püschel, C. Klingenberg, A. Elsler, F. Babarović and S. de Esteban-Trivigno for insight and discussion on the methods. We thank Ó. Sanisidro and L. Balsa Pascual for design and technical advice that greatly improved the quality of the graphic support. G.N. was supported by a PG Scholarship/Studentship from the Alumni Foundation, University of Bristol, UK, and is currently supported by the ERC project ‘TEMPO’ (grant number 639791). J.M.-L. is supported by the Spanish MINECO, Project CGL-2013-42643. E.J.R. and J.A.B. were supported by BBSRC grant number BB/I011668/1. C.R.C. is supported by a Leverhulme Early Career Fellowship (grant number ECF-2018-101).

Author contributions

The focus and design of this research were developed by G.N., J.M.-L., J.A.B. and E.R.J. C.R.C. conducted the VRMAs. G.N. conducted the remaining analyses. G.N., J.M.-L., J.A.B., C.R.C. and E.R.J. wrote the manuscript.

Competing interests

The authors declare no competing interests.

Additional information

Extended data is available for this paper at <https://doi.org/10.1038/s41559-019-1092-y>.

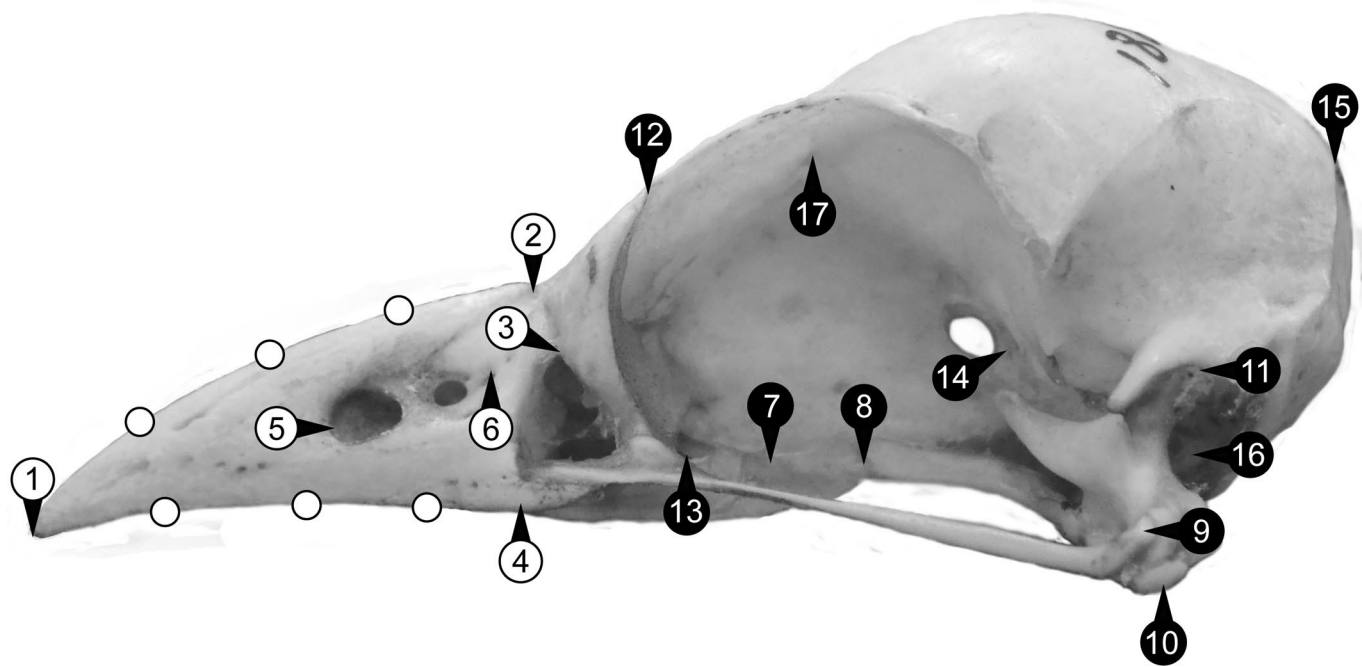
Supplementary information is available for this paper at <https://doi.org/10.1038/s41559-019-1092-y>.

Correspondence and requests for materials should be addressed to G.N. or E.J.R.

Reprints and permissions information is available at www.nature.com/reprints.

Publisher’s note Springer Nature remains neutral with regard to jurisdictional claims in published maps and institutional affiliations.

© The Author(s), under exclusive licence to Springer Nature Limited 2020

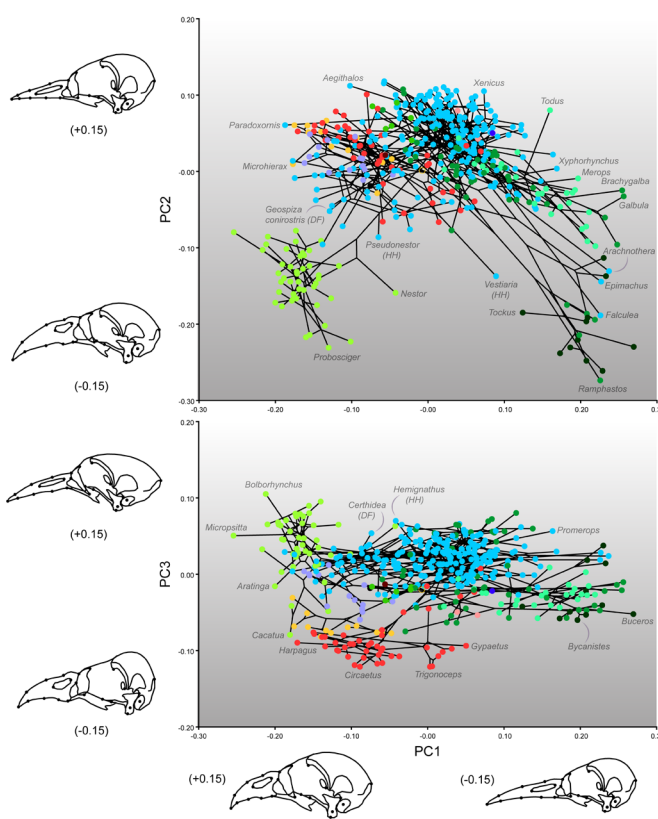
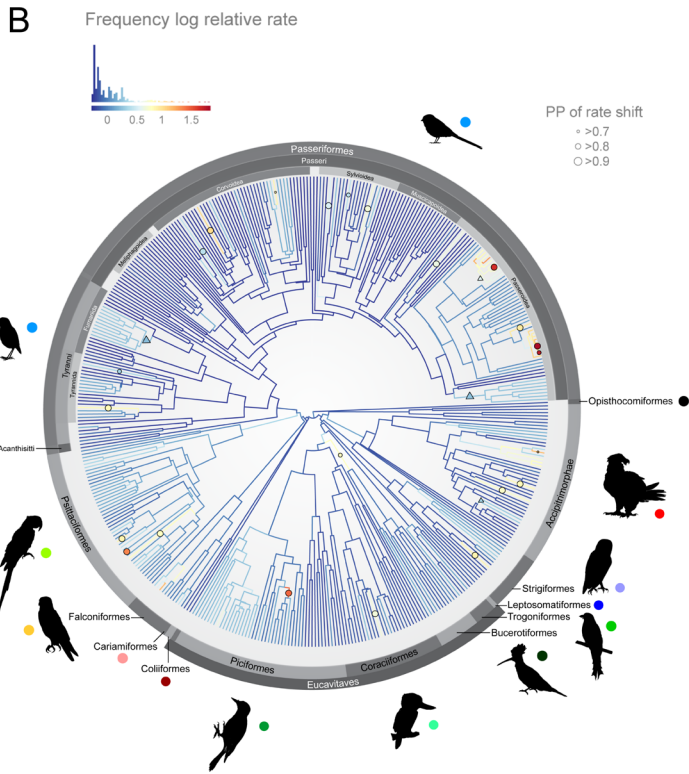


Extended Data Fig. 1 | Landmarks and semilandmarks used in this study for the beak (white) and skull (black) blocks. Landmark definition in Extended Data Table 1.

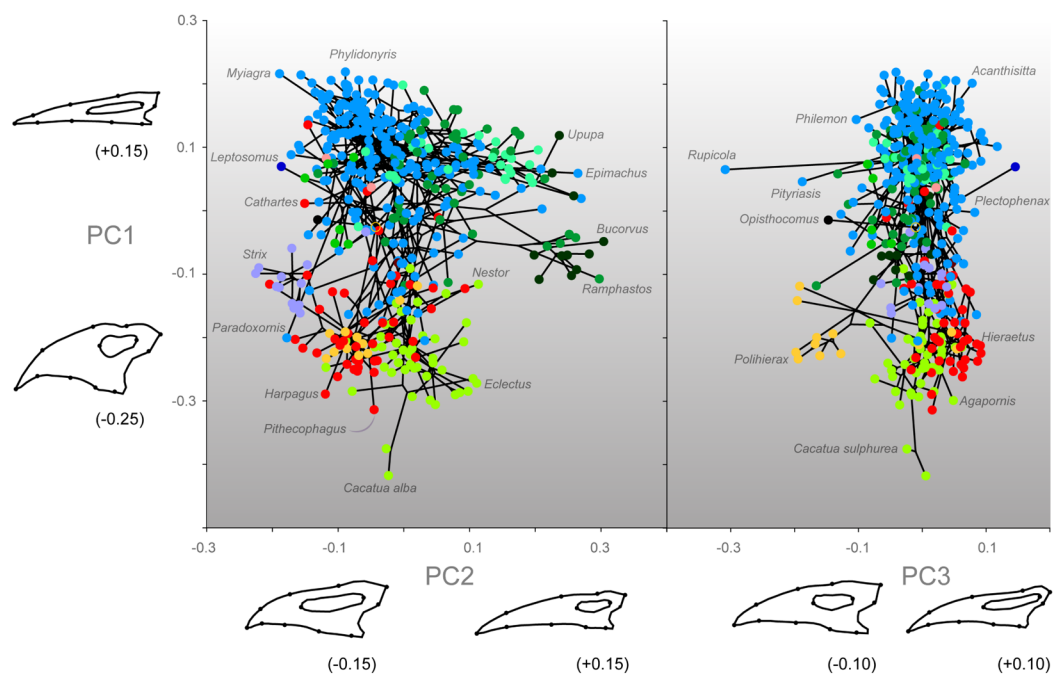
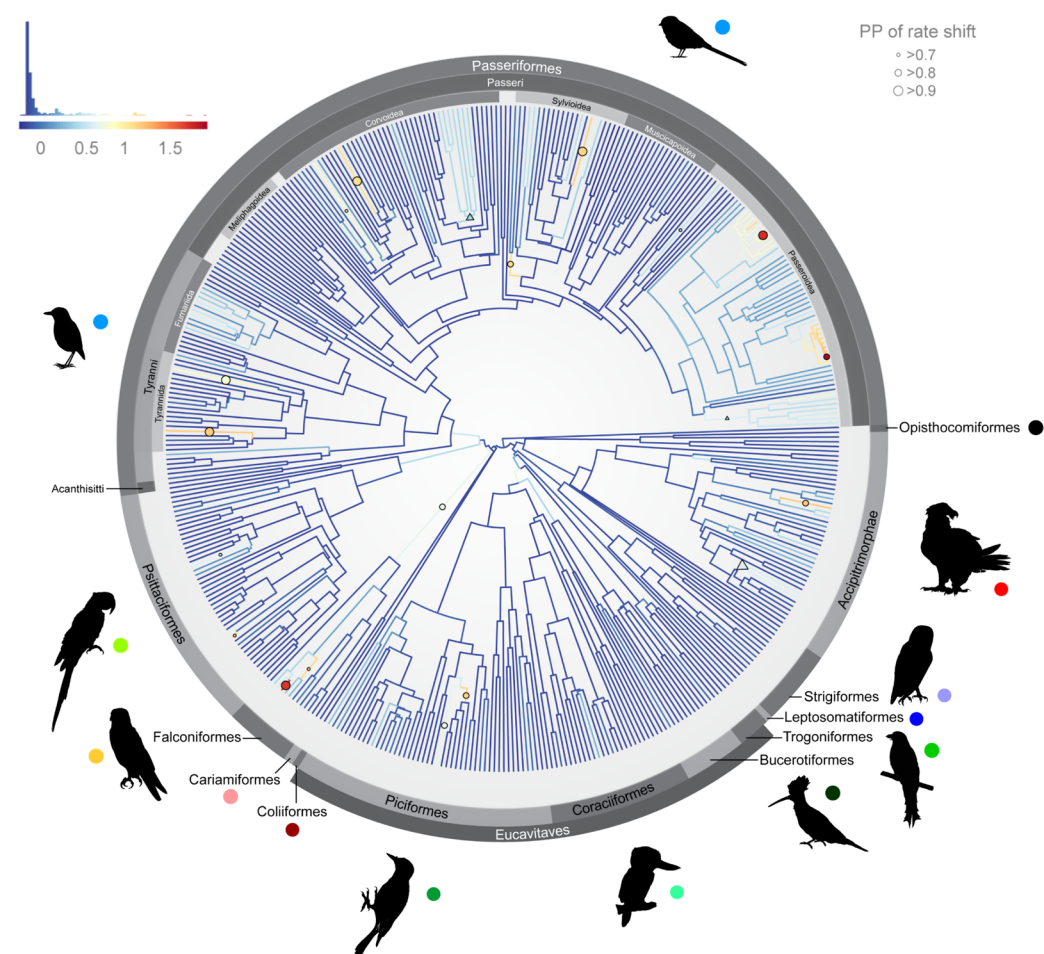
N	Block	Anatomical region	Description
1	Beak	Rostrum	Anterior tip of the premaxillary symphysis
2	Beak	Rostrum	Nasofrontal hinge
3	Beak	Rostrum	Ventrolateral end of the contact between nasal and lacrimal (or lacrimal-ectethmoid complex**)
4	Beak	Rostrum	Anteriormost edge of antorbital fossa orthogonally projected to the ventral rim of the maxilla
5	Beak	Rostrum	Anteriormost point of external naris fossa
6	Beak	Rostrum	Posteriormost point of external naris fossa
7	Skull	Palate	Middle point of the medial contact between palatines
8	Skull	Palate	Middle point of the lateral contact of palatine and pterygoid
9	Skull	Quadratoquadrate	Medial condyle of quadrate
10	Skull	Quadratoquadrate	Contact of jugal bar and quadrate
11	Skull	Quadratoquadrate	Lateral contact of ootic process of quadrate and squamosal
12	Skull	Lacrimal-ectethmoid	Posterolateral tip of lacrimal (or lacrimal-ectethmoid complex**)
13	Skull	Lacrimal-ectethmoid	Posterolateral end of the contact between lacrimal (or lacrimal-ectethmoid complex**) and frontal
14	Skull	Neurocranium	Ventralmost point of the foramen of the optic nerve
15	Skull	Neurocranium	Intersection of <i>crista nuchalis transversus</i> and <i>crista nuchalis sagittalis</i>
16	Skull	Neurocranium	External ear (geometric centre of the auditory meatus)
17	Skull	Neurocranium	Foramen of the olfactory nerve (geometric centre)
18-21	Beak	Rostrum	Curve 1 of three semilandmarks along the beak culmen
21-24	Beak	Rostrum	Curve 2 of three semilandmarks along the right tomial ridge

** term coined by Cracraft¹ to describe the coordinated evolution of both bones in modern birds which we used for the purposes of landmarking.

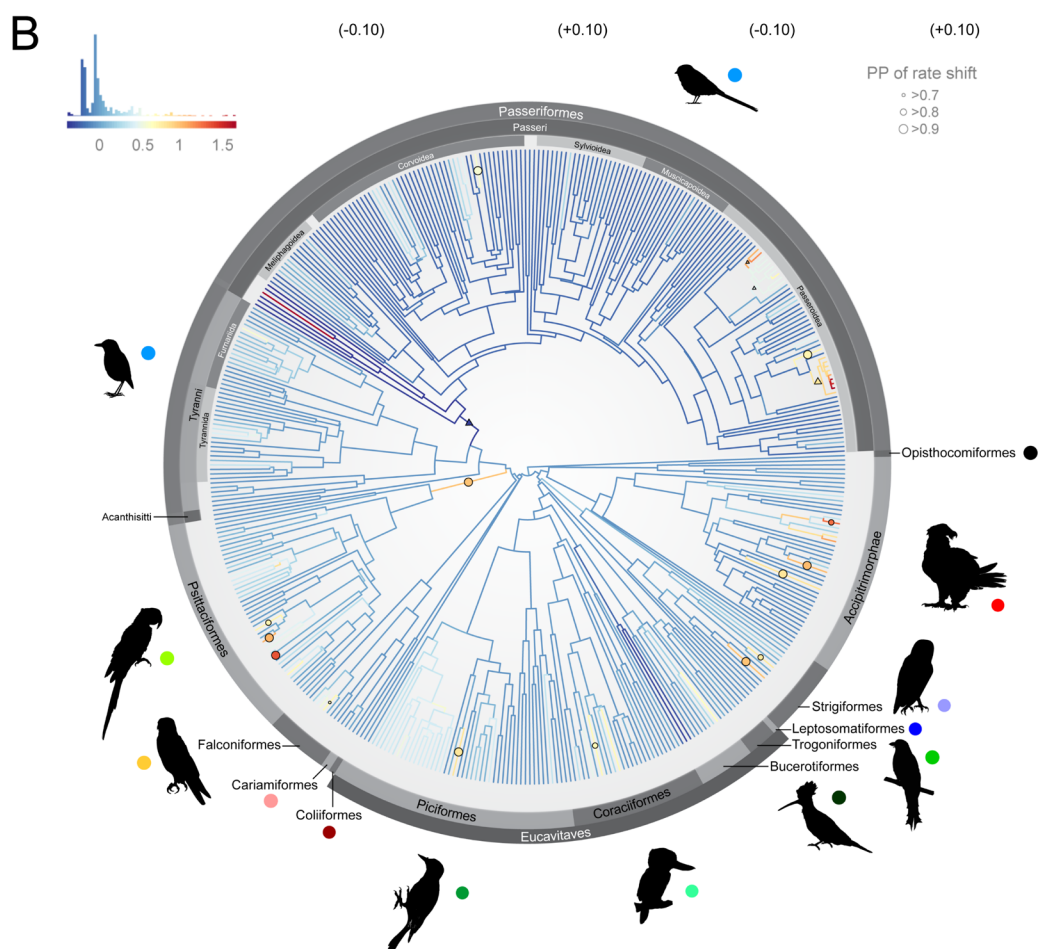
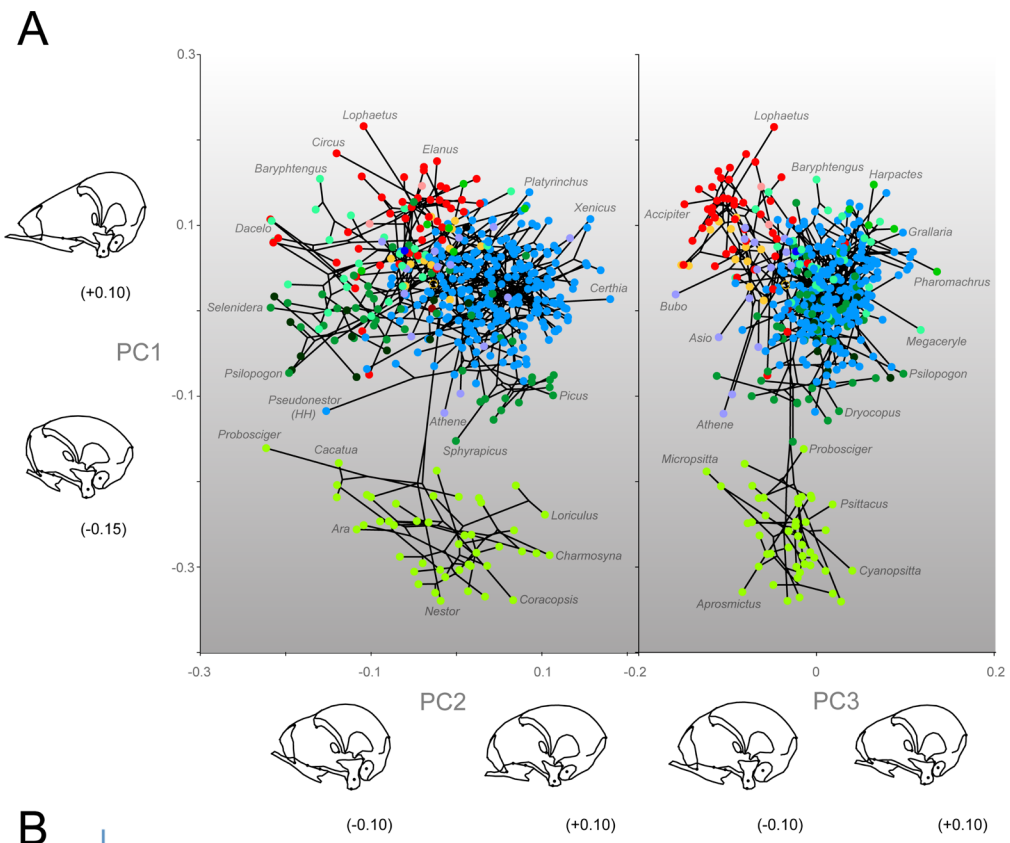
Extended Data Fig. 2 | Landmarks used in this study. **Cracraft, J. The lacrimal-ectethmoid bone complex in birds: a single character analysis. *American Midland Naturalist*, 316-359 (1969).

A**B**

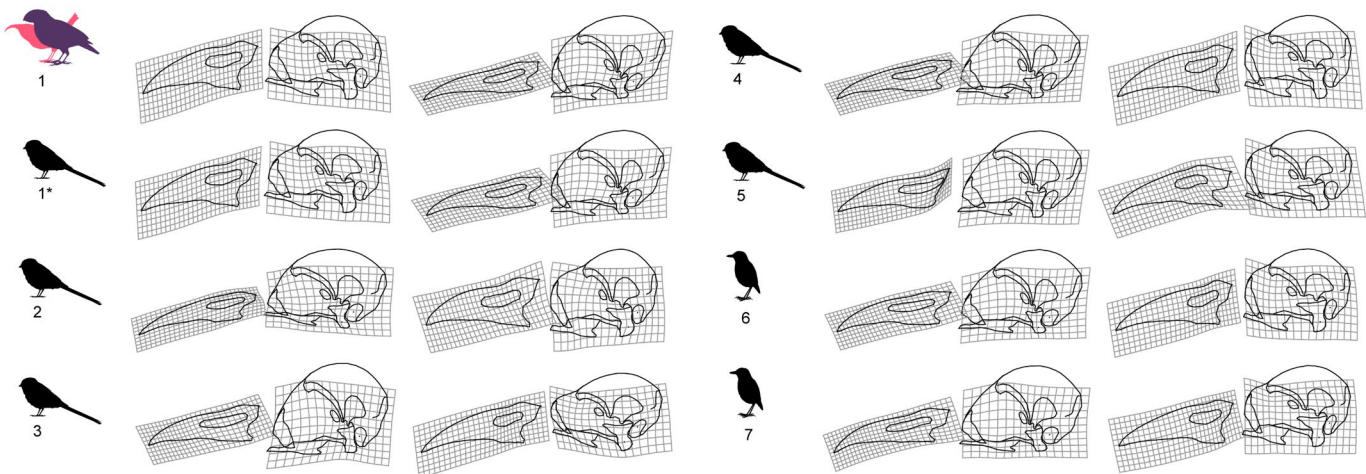
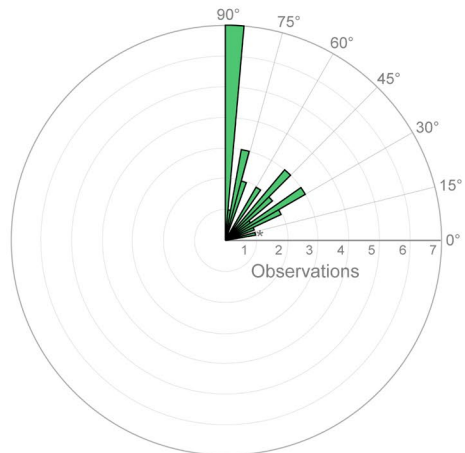
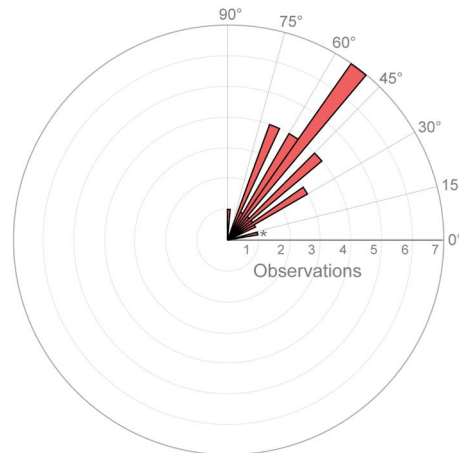
Extended Data Fig. 3 | Tempo and mode of craniofacial shape evolution in landbirds (labelled by major radiations). Phylomorphospaces of the first three PCs (**a**) and rates of evolution (**b**) for the whole skull configurations. Dot colours in phylomorphospaces (**a**) correspond to each major landbird lineage (colour legend by each silhouette in **B**). Branch colours in **B** indicate relative rate of shape evolution. Inferred rate shifts with higher posterior probability than 0.7 are plotted in corresponding branches (circles) or nodes (triangles) in the phylogeny in **B**. Posterior probability of each inferred rate shift is indicated by size as indicated in the legend in **b**.

A**B**

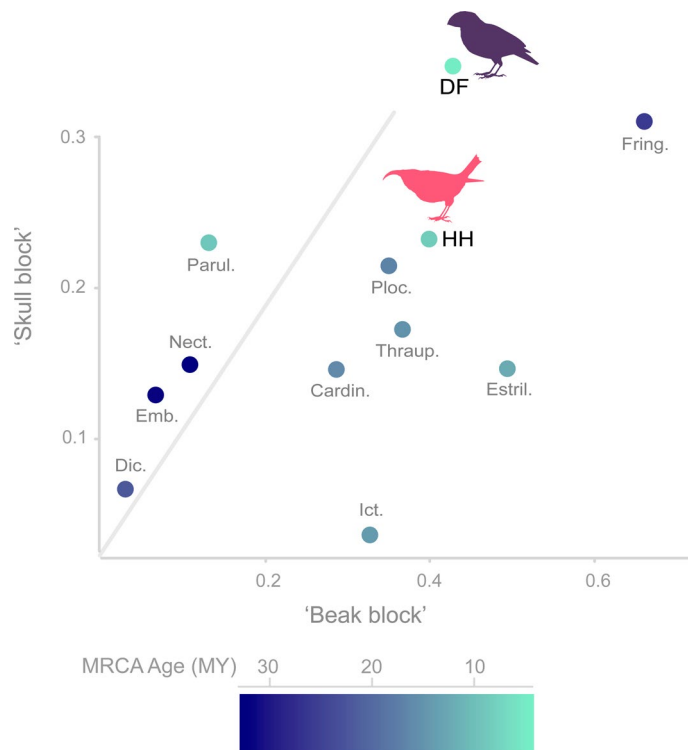
Extended Data Fig. 4 | Tempo and mode of beak shape evolution in landbirds (labelled by major radiations). Phylomorphospaces of the first three PCs (a) and rates of evolution (b) for the beak block configurations. Colours and legends as before.



Extended Data Fig. 5 | Tempo and mode of skull shape evolution in landbirds (labelled by major radiations). Phylomorphospaces of the first three PCs (a) and rates of evolution (b) for the skull block configurations. Colours and legends as before.

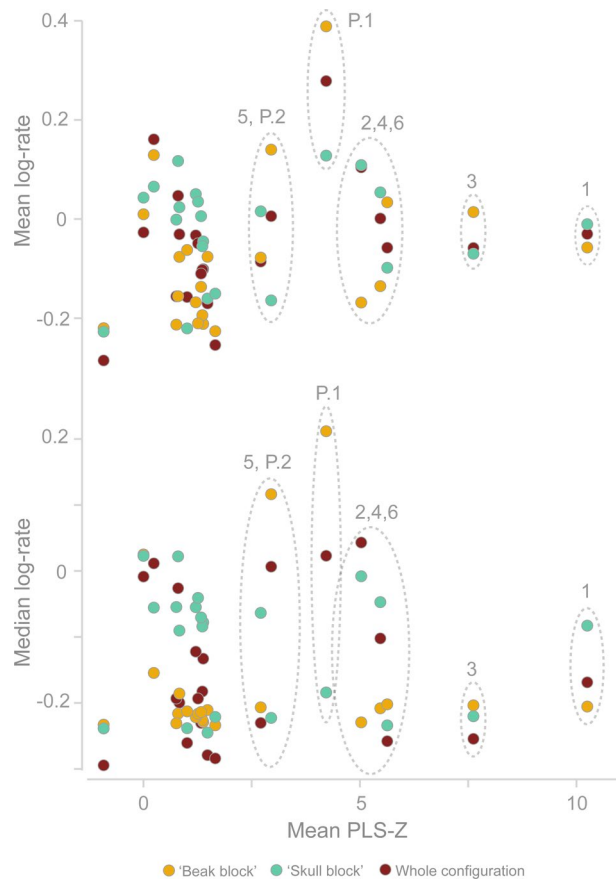
A**B****C**

Extended Data Fig. 6 | Shape differences associated with the first pair of PLS vectors (PLS1) for the beak block and the skull block for the main lineages of passerines. Polar histograms summarizing angle comparisons between the PLS1 vectors for the beak (**b**) and skull (**c**) blocks. As orientation of PLS1 vectors is arbitrary, the maximum possible angle between PLS1 vectors is 90°. * indicates single angular comparison of the PLS1 vectors of Passeroidea excluding DF and HH.



Extended Data Fig. 7 | Extreme morphologies and spread along lines of least resistance for each family within the parvorder Passeroidea in our sample.

Within-family maximum Procrustes distances for PLS1scores (situation 2) for both beak and skull blocks. Done for all the families that include two or more species in our sample. Legend for labels in Extended Data Table 2. Dot colours correspond to the ages of the most common recent ancestor (MRCA) for each of the focal families in our MCC tree.



Extended Data Fig. 8 | Relationship between levels of cranial integration and evolutionary rates per clade. Dotplot showing the relationship between mean and median log-rate per landbird/passine clade (clades as defined in Figs. 3, 4 and Table 1) with mean clade zscore values (that is evolutionary covariation, situation 2). Dashed ellipses encompass the values for selected clades: 1, All landbirds; 2, Non-passines; 3, Passeriformes; 4, Passeri; 5, Tyranni; 6, Psittaciformes; P.1, Passeroidea (including Darwin's finches and Hawaiian honeycreepers); P.2, Passeroidea (excluding Darwin's finches and Hawaiian honeycreepers).

Label	Family
Acanth.	Acanthisittidae
Acc.	Accipitridae
Alaud.	Alaudidae
Alced.	Alcedinidae
Brachyp.	Brachypteraciidae
Buc.	Bucerotidae
Bucc.	Bucconidae
Cacat.	Cacatuidae
Cardin.	Cardinalidae
Cath.	Cathartidae
Cistic.	Cisticolidae
Corac.	Coraciidae
Corv.	Corvidae
Coting.	Cotingidae
Crac.	Cracticidae
DF	Darwin's finches (Geospizinae, Thraupidae)
Dic.	Dicaeidae
Ember.	Emberizidae
Estril.	Estrildidae
Euryl.	Eurylaimidae
Falc.	Falconidae
Fring.	Fringillidae (excluding Hawaiian honeycreepers)
Furn.	Furnariidae
Galb.	Galbulidae
HH	Hawaiian honeycreepers (Drepanidinae, Fringillidae)
Hirun.	Hirundinidae
Ict.	Icteridae
Lyb.	Lybiidae
Megal.	Megalaimidae
Melip.	Meliphagidae
Merop.	Meropidae
Momot.	Momotidae
Nect.	Nectariniidae
Paradi.	Paradisaeidae
Parul.	Parulidae
Phoen.	Phoeniculidae
Pic.	Picidae
Pipr.	Pipridae
Pitt.	Pittidae
Ploc.	Ploceidae
Psitt.	Psittacidae
Ptilon.	Ptilonorhynchidae
Ramph.	Ramphastidae
Strig.	Strigidae
Sturn.	Sturnidae
Sylv.	Sylviidae
Tham.	Thamnophilidae
Thraup.	Thraupidae (excluding Darwin's finches)
Timal.	Timaliidae
Tity.	Tityridae
Trog.	Trogonidae
Tyran.	Tyrannidae
Vang.	Vangidae

Extended Data Fig. 9 | Legend for family names. Fig. 4c, d and Extended Data Figure 6.

Θ			
BEAK	Passeriformes	Passeri	Tyranni
Passeroidea	27.57	23.17	44.37
Passeroidea*	31.35	28.70	43.59
Muscicapoidea	71.24	70.33	82.03
SKULL			
Passeroidea	30.98	27.51	41.32
Passeroidea*	33.69	29.63	43.42
Muscicapoidea	56.16	58.51	60.18

Extended Data Fig. 10 | Comparisons of the pattern of maximum covariation lines between Passeroidea and other selected passerine clades. Angles (θ , degrees) for each pair of PLS1 vectors for the beak and skull block in situation 2 between Passeroidea (including and excluding DF and HH), Muscicapida (the parvorder that includes the passerine radiations sympatric to DF and HH) and Passeriformes, Passeri (all oscine passerines) and Tyranni (all suboscine passerines). As orientation of PLS1 vectors is arbitrary, the maximum possible angle between PLS1 vectors is 90°. * excluding DF and HH.

Reporting Summary

Nature Research wishes to improve the reproducibility of the work that we publish. This form provides structure for consistency and transparency in reporting. For further information on Nature Research policies, see [Authors & Referees](#) and the [Editorial Policy Checklist](#).

Statistics

For all statistical analyses, confirm that the following items are present in the figure legend, table legend, main text, or Methods section.

n/a Confirmed

- The exact sample size (n) for each experimental group/condition, given as a discrete number and unit of measurement
- A statement on whether measurements were taken from distinct samples or whether the same sample was measured repeatedly
- The statistical test(s) used AND whether they are one- or two-sided
Only common tests should be described solely by name; describe more complex techniques in the Methods section.
- A description of all covariates tested
- A description of any assumptions or corrections, such as tests of normality and adjustment for multiple comparisons
- A full description of the statistical parameters including central tendency (e.g. means) or other basic estimates (e.g. regression coefficient) AND variation (e.g. standard deviation) or associated estimates of uncertainty (e.g. confidence intervals)
- For null hypothesis testing, the test statistic (e.g. F , t , r) with confidence intervals, effect sizes, degrees of freedom and P value noted
Give P values as exact values whenever suitable.
- For Bayesian analysis, information on the choice of priors and Markov chain Monte Carlo settings
- For hierarchical and complex designs, identification of the appropriate level for tests and full reporting of outcomes
- Estimates of effect sizes (e.g. Cohen's d , Pearson's r), indicating how they were calculated

Our web collection on [statistics for biologists](#) contains articles on many of the points above.

Software and code

Policy information about [availability of computer code](#)

Data collection	tpsDig.2, tpsRelw, TreeAnnotator (Beast2), MorphoJ (v.1.0.6), Resistant Procrustes Software (available online at: https://sites.google.com/site/resistantprocrustes/).
Data analysis	MorphoJ(v.1.0.6), R statistical environment (geomorph v.3.0.7.), BayesTraits V2.0.2.

For manuscripts utilizing custom algorithms or software that are central to the research but not yet described in published literature, software must be made available to editors/reviewers. We strongly encourage code deposition in a community repository (e.g. GitHub). See the Nature Research [guidelines for submitting code & software](#) for further information.

Data

Policy information about [availability of data](#)

All manuscripts must include a [data availability statement](#). This statement should provide the following information, where applicable:

- Accession codes, unique identifiers, or web links for publicly available datasets
- A list of figures that have associated raw data
- A description of any restrictions on data availability

All relevant raw data (landmark data and phylogenies) will be made available via the University of Bristol's DataBris repository. All the R code used in this article will be made available via the University of Bristol's DataBris repository.

Field-specific reporting

Please select the one below that is the best fit for your research. If you are not sure, read the appropriate sections before making your selection.

- Life sciences Behavioural & social sciences Ecological, evolutionary & environmental sciences

For a reference copy of the document with all sections, see nature.com/documents/nr-reporting-summary-flat.pdf

Ecological, evolutionary & environmental sciences study design

All studies must disclose on these points even when the disclosure is negative.

Study description

Using a sample of 436 bird species across virtually all families of landbirds (i.e: Inopinaves, defined as Telluraves + Opisthomocomus hoazin, Prum et al. 2015) and state-of-the-art geometric morphometrics and phylogenetic comparative methods, we quantify evolutionary interdependence between the bird beak and braincase (cranial integration) in every avian lineage to test whether this condition promotes or constrains evolution. We find high levels of integration across most clades of landbirds. Even more surprisingly, we find that the two textbook examples of adaptive radiations in birds, Darwin's finches and Hawaiian honeycreepers, rapidly evolved a large range of beak shapes despite tight cranial integration. This is highly unexpected. We show that, contrary to conventional thinking, tight cranial integration actually facilitated, rather than constrained, diversification in two of the archetypal examples of adaptive radiation.

Research sample

Our study includes 128 families of landbirds giving a total of 436 species. All but five families within the landbird radiation are represented in our sample (Philepittidae, Sapayoaidae, Dasyornithidae, Urocynchramidae and Aegithinidae). These families are either monotypic or have an extremely reduced diversity, and often regarded as belonging within other passerine families 44. Sampling was non-random and aimed to capture the maximum beak morphological disparity within each family, with a special focus on Darwin's finches and Hawaiian honeycreepers (represented in our sample by ~70% and ~ 60 % of their extant diversity, respectively).

Sampling strategy

Sampling was non-random and aimed to cover all the known families of landbirds (Inopinaves). Furthermore, a previously crowd-sourced sample of beak shapes was used aimed to capture maximum beak shape disparity within each of the studied families. One specimen per species was used as the focus of our study is macroevolutionary (between species).

Data collection

Skulls were photographed following standard procedures in macrophotography to ensure minimal distortion. Landmark data was collected using these photographs and standard software in geometric morphometrics. Shape data was extracted from this landmark data following state-of-the-art procedures in geometric morphometrics. All technical details are given in the Methods section of the article.

Timing and spatial scale

Museum specimens were photographed over the years 2015, 2016 and 2017 during at least ten visits to the skeletal collections of ornithology of the National History Museum (Tring, UK) and the Smithsonian National Museum of Natural History (Washington, D.C., USA).

Data exclusions

No data was excluded.

Reproducibility

All the analyses were repeated more than once to verify the methodological procedures were correct. Proof of this could be submitted upon request. Furthermore, our data is analyzed using three different analytical situations to stress the importance of some issues in the correctly quantification of trait covariation using current methods in geometric morphometrics and phylogenetic comparative methods. We propose a pipeline to identify and novel solutions to solve these issues.

Randomization

This is not relevant to our study. Bird species were assigned to the clades in which they are recovered in our phylogenetic hypothesis (maximum clade credibility tree from a population of trees produced by a previous and large phylogenomic study).

Blinding

This is not relevant to our study. Only the first author, G.N., collected the data.

Did the study involve field work? Yes No

Reporting for specific materials, systems and methods

We require information from authors about some types of materials, experimental systems and methods used in many studies. Here, indicate whether each material, system or method listed is relevant to your study. If you are not sure if a list item applies to your research, read the appropriate section before selecting a response.

Materials & experimental systems

n/a	Involved in the study
<input checked="" type="checkbox"/>	Antibodies
<input checked="" type="checkbox"/>	Eukaryotic cell lines
<input checked="" type="checkbox"/>	Palaeontology
<input checked="" type="checkbox"/>	Animals and other organisms
<input checked="" type="checkbox"/>	Human research participants
<input checked="" type="checkbox"/>	Clinical data

Methods

n/a	Involved in the study
<input checked="" type="checkbox"/>	ChIP-seq
<input checked="" type="checkbox"/>	Flow cytometry
<input checked="" type="checkbox"/>	MRI-based neuroimaging